Structure and energetics of helium films on alkali substrates

Massimo Boninsegni
Department of Physics, University of Alberta, Edmonton, Alberta, Canada T6G 2J1

Leszek Szybisz
Laboratorio TANDAR, Departamento de Física, CNEA, Buenos Aires, Argentina
and Departamento de Física, FCEyN, Universidad de Buenos Aires, and CONICET, Argentina
(Received 25 March 2004; published 21 July 2004; publisher error corrected 23 July 2004)

Low-temperature adsorption of ^{4}He films on Alkali metal substrates is investigated theoretically by means of ground-state quantum Monte Carlo simulations. The most accurate potentials currently available are utilized to model the interaction of ^{4}He atoms with the substrate. Continuous growth of film thickness as a function of chemical potential is observed on Li, Na, and K substrates. A superfluid monolayer forms on a Li substrate; on Na and K, thermodynamically stable films are a few layers thick. The uncertainties of the calculation and in the potentials, preclude a definitive conclusion on the existence of a stable ^{4}He film on Rb. A comparison of the results of this calculation with those obtained using the Orsay-Trento density functional shows broad quantitative agreement.

DOI: 10.1103/PhysRevB.70.024512 PACS number(s): 67.70.+n, 61.30.Hn, 68.08.Bc

I. INTRODUCTION

The investigation of helium films adsorbed on different substrates is a subject of considerable fundamental interest, owing to the unusual, often intriguing physical properties that these films display.[1] A chief example is the rich phase diagram of helium on graphite, which has been the subject of an intense investigation over the past three decades.

A significant effort has also been devoted to the experimental characterization of helium films on weakly attractive substrates, such as those of alkali metals,[2–15] following original suggestions that, at low temperature, the weakness of the adsorption potential may result in novel physics.[16,17] Some of the main predictions have been experimentally confirmed; for example, a wetting transition for ^{4}He has been observed on Cs,[2,3] whereas intriguing superfluid behavior has been reported[14] on Rb.

Early microscopic theoretical studies of adsorption of ^{4}He on these substrates, based on realistic potentials, have been carried out by means of density functional (DF) methods. Density functional theory (DFT) provides a theoretical framework allowing, in principle, the exact calculation of ground state expectation values for quantum many-body systems. In practice, however, any DF approach requires a heuristic *ansatz* for the unknown functional expressing the ground-state energy of the system as a function of the ^{4}He density $\rho(\mathbf{r})$. Two approaches have been proposed, differing in the way the correlation term in the energy DF is represented (see, for instance, Ref. 17). One is essentially a variational method, based on the hypernetted chain approximation combined with the use of a correlated basis function.[18,19] An alternative procedure consists of writing down a parametric expression for the energy DF, with parameters adjusted so that some bulk properties of superfluid ^{4}He are reproduced quantitatively.[20,21] The latter approach has been more widely used in recent times to investigate ^{4}He adsorption on alkali metal substrates,[22–25] particularly with the most recent adatom-substrate potentials.[26] Although DF techniques have been, over the course of the years, refined to a remarkable level of sophistication, they remain to some extent uncontrolled. Thus, it makes sense to carry out a quantitative check of their predictions by means of an alternative computational method.

Path integral Monte Carlo (PIMC) simulations are the obvious choice, as they afford the accurate calculation of thermodynamic properties of interacting quantum many-body systems, with virtually no approximation, and no need for any *ad hoc* assumption. This method has a long history of successful application to the study of the superfluid transition in ^{4}He (see Ref. 27), and has also been used to investigate a variety of quantum fluids in confinement, including ^{4}He films on simple model alkali substrates.[28,29] The main shortcoming of PIMC is possibly the fact that calculations can be computationally expensive; the typical size of a sample of ^{4}He fluid that can be investigated numerically, is only a few hundred atoms. In practice, however, this does not prove too serious a limitation for the determination of energetics and most of the main structural properties of bulk systems.

In previous work, some limited comparisons of results for adsorbed ^{4}He films on selected alkali substrates, computed by DF and PIMC (or, by other quantum Monte Carlo techniques) were carried out.[23,29,30] To some extent, however, these comparisons are less than systematic; for example, in some cases different potentials were utilized to model the interaction between helium atoms and the substrate. Furthermore, whereas DF results are at $T=0$, PIMC estimates are at finite temperature. Although one can still obtain ground state estimates by performing calculations at different low temperatures and extrapolating the results to $T=0$, such a procedure can be quite lengthy and is generally avoided. Typically, results are provided at just one temperature, believed sufficiently low (e.g., $T\approx 0.5$ K) that the system is essentially in the ground state.

The goal of this work is to provide accurate numerical ground-state estimates for structure and energetics of ^{4}He

films on lithium (Li), sodium (Na), potassium (K), and rubidium (Rb) substrates. In order to make such a comparison as direct as possible, we utilize a variant of PIMC, known as variational path integral (VPI), which provides *ground-state* estimates, thus eliminating the need for extrapolation of low-temperature data.[27,31]

DF results quoted here are obtained with what has come to be known as the Orsay-Trento functional,[20] which has yielded interesting results for a variety of physical systems, including ^{4}He droplets and surfaces.[21] Some of the DF results have already appeared elsewhere.[23,25] All throughout, the most realistic models of the physical systems of interest are utilized, based on accurate potentials to describe both the interaction between helium atoms, as well as between these atoms and the substrate.

VPI results show stable ^{4}He films on Li, Na, and K substrates. In all these cases, there is no evidence of layering, but rather of continuous film growth as a function of the chemical potential. On Li, a stable superfluid monolayer is found, in agreement with a previous theoretical calculation based on a cruder model for the adatom-substrate interaction.[29] On Na and K substrates, the lowest coverages for which stable films form correspond to effective thicknesses of ~ 2 and ~ 4 layers. Finally, on a Rb substrate, VPI data presented here do not allow us to draw a definitive conclusion, regarding the occurrence of a stable adsorbed film at $T=0$. Circumstantial evidence seems to point to the existence of a stable film, but further work will be needed to consolidate this result, given the limited accuracy with which the potentials are presently known, as well as the statistical and systematic errors of the calculation. We did not investigate adsorption on a cesium substrate, on which a wetting transition has been observed experimentally with ^{4}He (as mentioned above).

In general, the agreement between VPI and DF results is quite satisfactory, eliciting confidence in the predictive power of state-of-the-art DF methods.

The remainder of this manuscript is organized as follows: in the next section, the model Hamiltonian is briefly introduced, whereas in the following section details of the computational method utilized (VPI) are presented (for an illustration of the DF methodology, the reader is referred to Refs. 21 and 23); we then illustrate our results and outline our conclusions.

II. MODEL

Consistently with all previous theoretical studies, our system of interest is modeled as an ensemble of N ^{4}He atoms, regarded as point particles, moving in the presence of an infinite, smooth planar substrate (positioned at $z=0$). The system is enclosed in a vessel shaped as a parallelepid, with periodic boundary conditions in all directions. Let A be the area of the substrate; correspondingly, the nominal ^{4}He coverage is $\theta=N/A$. The quantum-mechanical many-body Hamiltonian is the following:

$$\hat{H} = -\frac{\hbar^2}{2m}\sum_{i=1}^{N}\nabla_i^2 + \sum_{i<j} V(r_{ij}) + \sum_{i=1}^{N} U(z_i). \qquad (1)$$

Here, m is the ^{4}He atomic mass, V is the potential describing the interaction between two helium atoms, only depending on their relative distance, whereas U is the potential describing the interaction of a helium atom with the substrate, also depending only on the distance of the atom from the substrate. We use the accepted Aziz potential[32] to describe the interaction of two helium atoms, which has been used in almost all previous studies and has also been shown[27] to provide an accurate description of the energetics and structural properties of liquid ^{4}He in the superfluid phase.

The simplest model potential to describe the interaction of a helium atom with a smooth substrate [i.e., the U term in (1)] is the so-called 3-9 potential:

$$U_{3\text{-}9}(z) = \frac{4C^3}{27D^2z^9} - \frac{C}{z^3} \qquad (2)$$

which is a functional form obtained by integrating the Lennard-Jones potential over a semi-infinite, continuous slab. The parameters C and D are normally adjusted to fit the results of some *ab initio* electronic structure calculations for the specific adatom-substrate system of interest. Most of the early microscopic calculations were carried out using this potential. Successively, the following, more elaborate form (heretofore referred to as CCZ) was proposed by Chizmeshya, Cole, and Zaremba,[26] based on the original prescription of Zaremba and Kohn:[33]

$$U(z) = U_\circ(1+\alpha z)e^{-\alpha z} - \frac{C_{vdw} f_2\,(\beta(z)(z-z_{vdw}))}{(z-z_{vdw})^3} \qquad (3)$$

with $f_2(x)=1-e^{-x}(1+x+x^2/2)$ and $\beta(x)=\alpha^2 x/(1+\alpha x)$. The first term in (3) represents the Pauli repulsion between the electronic cloud of the He atom and the surface electrons, whereas the second term expresses the Van der Waals attraction. All of the results presented here (both the DF and VPI ones) are obtained using this potential, with the values of the parameters $U_\circ$, α, C_{vdw}, and z_{vdw} supplied in Ref. 26.

It is worth noting that, even with the more accurate CCZ potential (3), the model utilized here is, clearly, highly simplified. By far the most important simplification consists of the neglect of substrate corrugation, whose role is significant for attractive substrates, such as graphite,[34] but can be expected to be less important on substrates, such as those of Alkali metals, which are relatively weak.

III. METHODOLOGY

The variational path integral (VPI) method is a numerical (Quantum Monte Carlo) technique that allows one to obtain estimates, in principle exact, of ground-state expectation values for quantum many-body systems described by a Hamiltonian such as (1). The basic ideas are common to other projection techniques, such as diffusion (DMC) or Green function Monte Carlo (GFMC); however, VPI has the advantage of providing relatively easily expectation values for physical observables that do not commute with the Hamiltonian operator. Moreover, VPI is immune from the bias affecting DMC/GFMC, arising from the fact that one is working with a finite population of random walkers. Finally, although a trial wave function Ψ_T for the physical system of interest is required in VPI calculations (as in DMC or

GFMC) empirical evidence suggests[35] that results for observables other than the energy are considerably less sensitive to the choice of Ψ_T than in DMC or GFMC.

This is how it works: One generates sequentially, on a computer, a large set $\{X^m\}$, $m=1,2,\ldots,M$, of many-particle paths $X \equiv R_0 R_1 \ldots R_{2L}$ through configuration space. Each $R_j \equiv \mathbf{r}_{j1}\mathbf{r}_{j2}\ldots\mathbf{r}_{jN}$ is a point in $3N$-dimensional space, representing positions of the N particles (i.e., ^{4}He atoms) in the system. These paths are statistically sampled from a probability density

$$\mathcal{P}(X) \propto \Psi_T(R_0)\Psi_T(R_{2L})\left\{\prod_{j=0}^{2L-1} G(R_j,R_{j+1},\tau)\right\} \tag{4}$$

where $\Psi_T(R)$ is a variational wave function for the ground state of the system and $G(R,R',\tau)$ is a short-time approximation for the imaginary-time propagator $\langle R|\exp[-\tau\hat{H}]|R'\rangle$. Several choices are possible for G; in this work, the following formula was used,[36] which is accurate up to order τ^4:

$$G(R_j,R_{j+1},\tau) = \prod_{i=1}^{N} \exp\left[-\frac{m(\mathbf{r}_{ji}-\mathbf{r}_{j+1,i})^2}{2\hbar^2\tau}\right] \times \exp\left[-\frac{2\tau\mathcal{V}(R_j)}{3}\right]\rho_v(R_j) \tag{5}$$

where

$$\rho_V(R_j) = \exp\left[-\frac{2\tau\mathcal{V}(R_j)}{3} - \frac{\tau^2\hbar^2}{9m}\sum_{i=1}^{N}(\nabla_i\mathcal{V}(R_j))^2\right] \tag{6}$$

if j is odd, whereas $\rho_V(R_j)=1$ is j is even. Here, $\mathcal{V}(R)$ is the total potential energy of the configuration R, which includes both the helium–helium and helium-substrate contributions [i.e., the U and V terms in (1)].

It is a simple matter to show[27] that in the limits $\tau\to 0$, $L\tau\to\infty$, R_L is sampled from a probability density proportional to the square of the exact ground-state wave function $\Phi(R)$, *irrespective of the choice of* Ψ_T.[37] One can therefore use the set $\{R_L^m\}$ of "middle point" configurations R_L of the statistically sampled paths, to compute ground-state expectation values of thermodynamic quantities $F(R)$ that are diagonal in the position representation, simply as statistical averages, i.e.,

$$\langle\Phi|\hat{F}(R)|\Phi\rangle \approx \frac{1}{M}\sum_{m=1}^{M} F(R_L^m), \tag{7}$$

an approximate equality that becomes asymptoptically exact in the $M\to\infty$ limit. The ground-state expectation value of the energy can be obtained in several ways; it is particularly convenient to use the "mixed estimate"

$$\langle\Phi|\hat{H}|\Phi\rangle \approx \sum_{m=1}^{M}\frac{\hat{H}\Psi_T(R_1^m)}{\Psi_T(R_1^m)} \tag{8}$$

which provides an unbiased result for the Hamiltonian operator $\hat{H}$, as it commutes with the propagator $\exp[-\tau\hat{H}]$ [note that R_{2L} may just as well be used in Eq. (8)].

Because L is necessarily finite, for a given value of τ one must repeat the calculation for increasing L, until convergence of the estimates is achieved, within the desired accuracy. For any finite L, the energy expectation value is a strict upper bound for the exact value, hence the name *variational* path integral. A better choice of Ψ_T or a more accurate form for $G(R,R',\tau)$ (e.g., the pair product approximation of Pollock and Ceperley[27]), will allow one to observe convergence with a smaller value of L and/or a greater time step τ, but will not otherwise affect the results. Numerical extrapolation of the estimates obtained for different τ must then be carried out, in order to obtain results in the $\tau\to 0$ limit.

For a given choice of L and τ, one computes the approximate estimates (7) and (8) by generating the set $\{X^m\}$ by means of a random walk through path space, using the Metropolis algorithm. The same path sampling techniques utilized in finite temperature PIMC can be used in VPI. In this work, multilevel sampling with bisection and staging[27] was adopted, together with rigid displacements of entire single-particle paths. It is worth mentioning that the only difference between multilevel moves for central portions of the path and for those including the ends (i.e., "slices" 1 and $2L$) is the presence, in the latter, of the trial wave function Ψ_T in the Metropolis acceptance/rejection test. Other strategies have been proposed, allowing one to update paths in the vicinity of the ends, e.g., *reptation*-type moves;[38] however, in this work we have not made use of them.

The trial wave function Ψ_T utilized in this work has the following form:

$$\Psi_T(R) = \prod_{i=1}^{N} f(z_i)\prod_{i<j}\exp[-u(|\mathbf{r}_i-\mathbf{r}_j|)] \tag{9}$$

$f(z)$ is the exact ground-state wave function of a single ^{4}He atom in the presence of the substrate, obtained by solving Schroëdinger equation numerically for the different substrates considered. As for u, we took

$$u(r) = \frac{\alpha}{1+\beta r^5} \tag{10}$$

the optimal values for the variational parameters being, respectively, $\alpha=19$ and $\beta=0.12$ Å^{-5}, obtained for bulk liquid ^{4}He.

We have empirically observed convergence of our physical estimates using a projection time $L\tau\approx 2$ K^{-1}; the time step τ required to obtain an accurate value of the energy is ≈ 0.005 K^{-1}, whereas estimates for other quantities, such as film density profiles, can be usually obtained with a time step as much as four times larger.

For values of the ^{4}He coverage $\theta \leqslant \theta_\circ = 0.076$ Å^{-2}, VPI calculations are carried out on a system of 36 helium atoms, initially arranged on a triangular lattice at a distance of 3 Å from the substrate. As the coverage is increased, and second-layer promotion is observed, the initial arrangement is taken to be a series of successive solid (triangular) layers of 2D density $\theta_\circ$, with an incomplete top layer. In all calculations, the height of the simulation box (i.e., the distance between the periodically replicated images of the substrate) is 40 Å, i.e., much greater than the maximum film thickness ob-

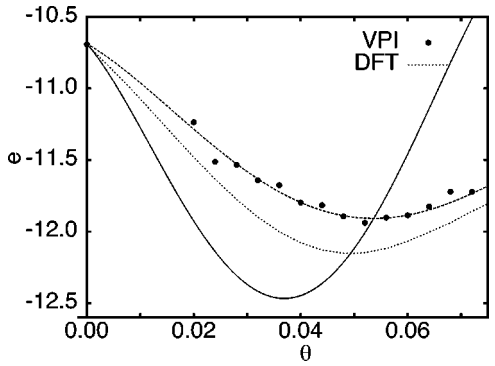

FIG. 1. Ground state energy per atom e (in K) versus coverage θ(Å^{-2}), for an adsorbed ^{4}He film on a Li substrate. Dashed line is a polynomial fit to the VPI data (filled circles), whereas the dotted line represents DFT estimates for e. Solid line is the chemical potential μ, computed using Eq. (13) and the fit to the values $e(\theta)$ obtained by VPI. Statistical errors on the VPI data are of the order of the symbol size.

served, so as to make the use of periodic boundary conditions in the z direction (perpendicular to the substrate) ininfluent. The largest system for which simulation results are reported here consists of 135 atoms, for a coverage of 0.270 Å^{-2}.

Physical quantities of interest, besides the ground-state energy per atom, are the ^{4}He density profiles as a function of the distance z from the substrate, i.e.,

$$n(z) \equiv \frac{1}{A} \int dx\, dy\, \rho(x,y,z) \tag{11}$$

where $\rho(x,y,z)$ is the 3D ^{4}He density, as well as the angularly averaged, "reduced" pair correlation function $g(r)$, with $r=\sqrt{x^2+y^2}$ and

$$g(x,y) = \frac{1}{A\theta^2} \int dx'dy' n(x+x',y+y')n(x',y') \tag{12}$$

with $n(x,y)=\int dz\, \rho(x,y,z)$. The correlation function $g(r)$ is only directly accessible to VPI, not to DF calculations, and it provides a quantitative assessment of the 2D character of an adsorbed film; the more 2D an adsorbed film, the more closely $g(r)$ mimics the pair correlation function of a strictly 2D system of the same coverage.

It is worth ending this section repeating that estimates for these quantities obtained within VPI are *unbiased*, i.e., do not depend on the trial wave function utilized, in the limit $L\tau \to \infty$.

IV. RESULTS

A. Lithium

We discuss Li separately because adsorbed helium films display a quite distinct behavior on this substrate; some of the more general considerations, however, apply to other substrates as well.

Figure 1 shows ground-state energy per^{4}He atom $e(\theta)$, as a function of coverage. This was computed by both VPI simulations as well as by DFT. The results yielded by the two methods seem in reasonable agreement, at least in the range of coverages explored here. Both calculations give an exact result in the $\theta \to 0$ limit. At finite coverages, DFT consistently underestimates the energy of the helium atoms in the film, by a fraction of a K ($\sim$0.2 K at the equilibrium coverage). The difference is seen to decrease at greater coverages. From the computed $e(\theta)$ the chemical potential $\mu(\theta)$ can be inferred as

$$\mu(\theta) = e(\theta) + \theta \frac{de(\theta)}{d\theta}.. \tag{13}$$

Figure 1 also shows $\mu(\theta)$, obtained using a polynomial fit to the values of $e(\theta)$ computed by VPI.

The equilibrium coverage θ_e [corresponding to the condition $\mu(\theta_e)=e(\theta_e)$] as determined by VPI is $\theta_e = 0.052 \pm 0.002$ Å^{-2}, in quantitative agreement with the DFT estimate ($\approx$0.050 Å^{-2}). Our estimate for θ_e is slightly above that ($\approx$0.046 Å^{-2}) obtained in previous work,[28] in which the simpler 3-9 potential was used to model the adatom-substrate interaction. The greater value of θ_e found here is consistent with the deeper attractive well of the CCZ potential [Eq. (3)]. Otherwise, the main physical features of this adsorbate are in qualitative agreement with the results of the calculations carried out in Ref. 29, as shown below.

The chemical potential $\mu(\theta)$ is a monotonically increasing function above $\theta_s \approx 0.036$ Å^{-2} ($d\mu/d\theta$ vanishes at $\theta=\theta_s$, as shown in Fig. 1). This denotes continuous growth of film thickness, with absence of layering. Below θ_e, the film is metastable; while one can obtain a solution corresponding to a uniform film at arbitrarily low coverage, using DFT, VPI simulations consistently fail to produce a uniform film for $\theta < \theta_s$, i.e., in the region where $d\mu/d\theta < 0$. The coverage θ_s is normally referred to as *spinodal* and represents the lowest coverage to which a uniform film can be "stretched" (at *negative* pressure), before it breaks down into 2D clusters ("puddles"). Its value on a Li substrate, as determined in this work, is very close to that obtained for purely 2D ^{4}He in two separate studies, based on slightly different versions of the Aziz potential.[39,40]

Direct observation of the many-particle configurations generated by the VPI Monte Carlo algorithm (Fig. 2) at coverages below θ_s indeed shows such a breakdown of the film, with the formation of clusters of liquid. Because the substrate is smooth, these clusters are not pinned anywhere, i.e., the local density of fluid averaged over the course of the simulation is constant throughout the substrate. The symmetry-breaking character of the solution yielded by VPI is inferred from the following: (a) random snapshots of the system (Fig. 2) reveal consistent lack of uniformity, and (b) the correlation function $g(r)$ decays at long distances, as opposed to tending asymptotically to 1, as would be the case for a uniform system (Fig. 3). At very low coverages ($\theta \lesssim 0.020$ Å^{-2}) the function $g(r)$ acquires a nonzero value at the origin; this, combined with the decrease of $g(r)$ at large distance, provides an indication that the film is "beading up" on the substrate, i.e., forming droplets (with a nonzero contact angle with the substrate) rather than 2D puddles.

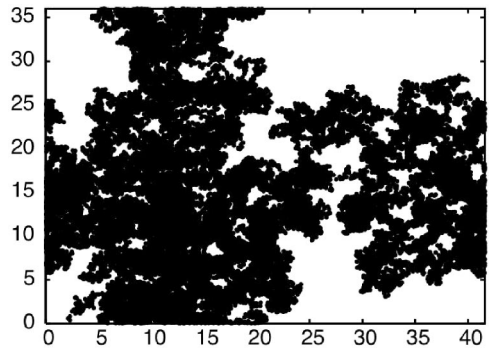

FIG. 2. Typical many-particle configuration for a ^{4}He film adsorbed on a Li substrate (top view), at a coverage of 0.024 Å^{-2}, generated by the VPI simulation. Each dot represents the position of one of 36 ^{4}He atoms at one of 1280 "imaginary time" slices utilized in the calculation. Periodic boundary conditions are used in both directions.

The breakdown of the simulated adsorbed film, which is observed at low θ on *all* substrates considered here, is in a sense remarkable, as the trial wave function utilized [Eq. (9)] is translationally invariant. As mentioned in Sec. III, however, one of the qualities of VPI is precisely its capability of furnishing physical results that are largely unaffected by the choice of trial wave function. While this is, in principle, true of other projection quantum Monte Carlo techniques, as long as unbiased estimators are used, in practice those methods based on imaginary-time diffusion of populations of walkers through configuration space (such as DMC) are more seriously affected by a particular choice of Ψ_T, i.e., lengthy simulations are often required in order to eliminate the variational bias.

At the equilibrium coverage θ_e, a stable monolayer liquid ^{4}He film is observed, whose physics is very nearly 2D. This can be established by examining the ^{4}He density profile $n(z)$ in the direction perpendicular to the substrate (see Fig. 4), for which DFT and VPI results compare quite well (as at other coverages, see Fig. 4). At $\theta=\theta_e$, a single adsorbed layer is present, with a width of approximately 2 Å.

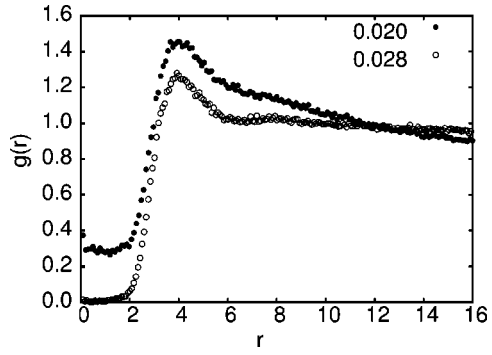

FIG. 3. Density correlation function $g(r)$, defined through Eq. (12), computed by VPI for a ^{4}He film adsorbed on a Li substrate, at coverages $\theta=0.020$ Å^{-2} (filled symbols) and $\theta=0.028$ Å^{-2} (open symbols). Statistical errors are of the order of symbol sizes. The finite value of $g(r)$ at the origin observed at the lower coverage is an indication of the film "beading up" on the substrate. Both curves display monotonic decay at long distances.

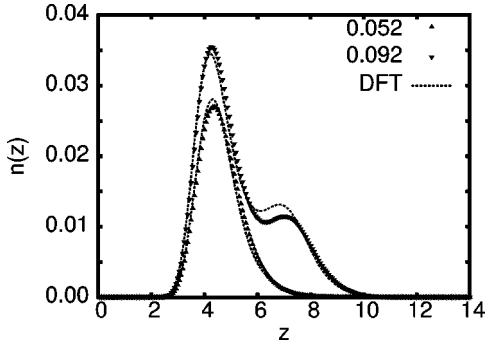

FIG. 4. Helium density profiles $n(z)$ (Å^{-3}) in the direction z(Å) perpendicular to a Li substrate. Filled symbols represent VPI data at the two coverages: 0.052 and 0.092 Å^{-2}. Statistical errors are smaller than the symbols. Dashed lines show the same profiles computed by DFT.

Even more telling is the density correlation function $g(r)$, defined in Eq. (12) and shown in Fig. 5. The computed $g(r)$ at $\theta=\theta_e$ is found to be quite similar to the pair correlation function in strictly 2D ^{4}He, at the same coverage.[41] These results confirm that this system may provide the closest experimental realization of a 2D superfluid.

The adsorbed ^{4}He monolayer is expected to undergo a superfluid (SF) transition at low temperature. The SF transition temperature T_c can be computed by finite temperature PIMC simulations. Based on the results shown here, as well as on the findings of Ref. 29, T_c can be expected to be the same as that of a strictly 2D film of the same coverage. Gordillo and Ceperley[40] carried out an extensive PIMC study of 2D ^{4}He, and found T_c to be very weakly dependent on θ. Thus, T_c is predicted here to be $\sim$760 mK, as in two dimensions; the thermodynamics of the SF transition has been shown[29] to conform quite closely to the Kosterlitz-Thouless (KT) paradigm.[42]

Second layer promotion, as evidenced by a nonzero value of $g(r\rightarrow 0)$, is observed at $\theta\approx 0.07$ Å^{-2}, i.e., at a coverage for which liquid and solid phases coexist, in the purely two-dimensional system.[40] This suggests that the adsorbed ^{4}He

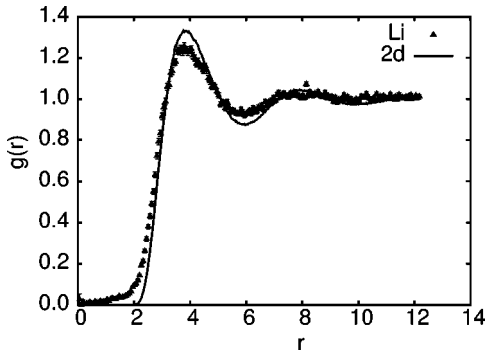

FIG. 5. Density correlation function $g(r)$, defined through Eq. (12), computed by VPI for a ^{4}He film adsorbed on a Li substrate, at the calculated equilibrium coverage $\theta_e=0.052$ Å^{-2}. Statistical errors are smaller than symbols. Solid line represents the pair correlation function computed for the ground state of 2D ^{4}He at the same coverage.

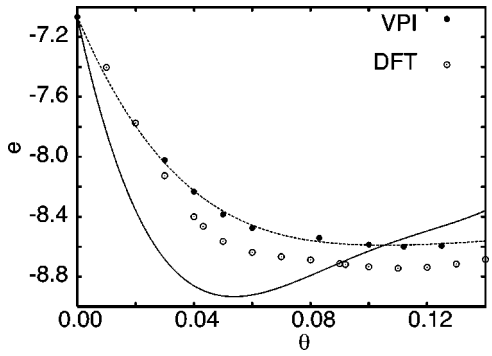

FIG. 6. Ground-state energy per atom e (in K) versus coverage θ (Å^{-2}) for an adsorbed ^{4}He film on a Na substrate, computed by VPI (filled circles) and DFT (open circles). Dashed line is a polynomial fit to the VPI data. Solid line is the chemical potential μ, computed using Eq. (13) and the fit to the values $e(\theta)$ obtained by VPI. Statistical errors on the VPI data are of the order of the symbol size.

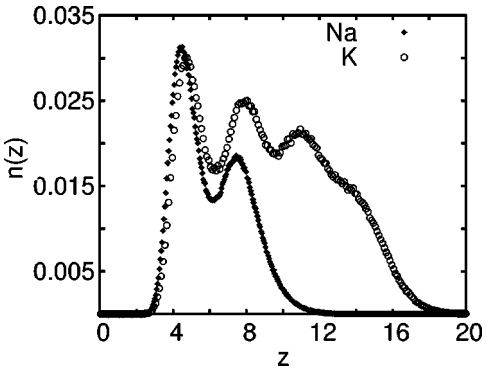

FIG. 7. Helium density profiles $n(z)$ (Å^{-3}) in the direction z(Å) perpendicular to a K (open symbols) and a Na (filled symbols) substrates computed by VPI (DFT results are identical on the scale of the figure and with the symbol sizes used). Results on Na are at a coverage $\theta=0.112$ Å^{-2}, on K at $\theta=0.240$ Å^{-2}. Statistical errors are of the order of the size of the symbols.

monolayer on Li undergoes no solidification, i.e., second-layer promotion occurs before the monolayer is compressed enough to solidify. As shown in Fig. 4, layers are poorly defined and overlap substantially, to suggest significant interlayer atomic exchange. This physical behavior is expected to occur, *a fortiori*, on weaker substrates as well.

B. Other substrates

Among the alkali metal substrates, sodium is the second most attractive. Figure 6 shows the ground-state energy per ^{4}He atom as a function of coverage, as well as the chemical potential, computed by fitting energy data obtained by VPI simulations (filled circles). The equilibrium coverage for this system is found to be $\theta_e=0.104\pm0.002$ Å^{-2}, which corresponds to roughly two layers (see comment below).

The VPI data, both for the energy as well as for the density profile, are in good quantitative agreement with the corresponding DFT results; just as in the case of Li, DFT underestimates the energy at finite coverage, the largest difference between the two calculations being of the order of $\sim$0.15 K. The equilibrium coverage determined by DFT is, in this case, approximately 0.11 Å^{-2}, the difference in energy between VPI and DFT data at such a coverage being of the order of 0.1 K, and decreasing for $\theta\geqslant\theta_e$. Just as for Li, the chemical potential is found to be a monotonically increasing function of θ above θ_e, indicating continuous growth of film, with no layering. This is in qualitative agreement with the density profile of Fig. 7, which displays two well-defined, but rather broad peaks. Here too, layers appear to be greatly overlapping.

The same general remarks can be made looking at the results on a potassium substrate, which is less attractive than sodium. The ground-state energy per ^{4}He atom is displayed in Fig. 8. A determination of the equilibrium coverage θ_e was not pursued; it is predicted by DFT to be in the neighborhood of 0.4 Å^{-2}, which corresponds to roughly four layers. Here too, DFT energy data are slightly below the VPI ones, but the difference is smaller than on the more attractive substrates; in fact, estimates obtained with VPI and DFT coincide, within the statistical errors of the VPI calculation, above $\theta\sim0.25$ Å^{-2}. Thus, we expect quantitative agreement between DFT and VPI, regarding the location of θ_e. Also, density profiles determined by DFT are in excellent agreement with those computed by VPI, above monolayer coverage (see Fig. 7).

In Ref. 29 numerical evidence was provided suggesting that, on a Li substrate, $T_c(\theta)$ should be a monotonically decreasing function for $\theta<\theta_e$, vanishing at $\theta=\theta_s$. The suggestion was made that, due to the weakness of the adsorption potential, superfluidity in the real system would cease to occur, in the low coverage limit, at the same value of θ found theoretically. In other words, the suppression of superfluidity would be due to an intrinsic instability of a 2D film, rather than due to a property of the substrate.

A superfluid transition is expected to occur on Na and K substrates as well because these adsorbed films are essentially 2D; the transition is still expected to be KT in charac-

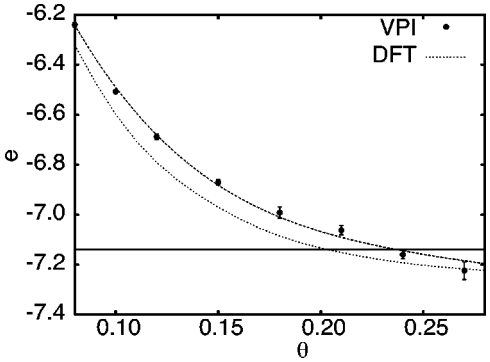

FIG. 8. Ground-state energy per atom e (in K) versus coverage θ (Å^{-2}) for an adsorbed ^{4}He film on a K substrate, computed by VPI (filled circles) and DFT (dotted line). Dashed line is a polynomial fit to the VPI data. Also shown for reference (solid line) is the chemical potential of equilibrium bulk ^{4}He at $T=0$ (-7.14 K). The value of $e(\theta)$ in the $\theta\rightarrow0$ limit is -4.21 K; DFT and VPI results coincide in that limit.

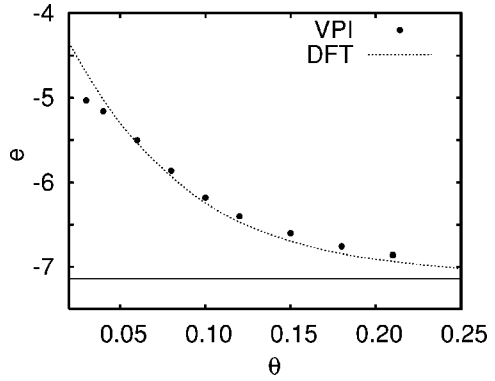

FIG. 9. Ground-state energy per atom e (in K) versus coverage $\theta(\text{Å}^{-2})$ for an adsorbed ^{4}He film on a Rb substrate, computed by VPI (filled circles) and DFT (dotted line). Also shown for reference (solid line) is the chemical potential of equilibrium bulk ^{4}He at $T=0$ (-7.14 K). The value of $e(\theta)$ in the $\theta \to 0$ limit is -3.72 K; DFT and VPI results coincide in that limit.

ter. These substrates are weaker than Li. We, therefore, predict that $T_c(\theta)$ will display the same behavior on these substrates as seen on Li; specifically it will vanish at the spinodal coverage, which is found here to be $\theta_s \sim 0.055$ Å^{-2} for Na, and $\theta_s \sim 0.13$ Å^{-2} for K.

In Fig. 8 the value is also shown (solid horizontal line) of the chemical potential μ_o of equilibrium bulk ^{4}He at $T=0$, which is approximately -7.14 K, obtained with the Aziz potential for helium utilized here.[43] The binding energy $\delta\epsilon$ of a ^{4}He atom in an adsorbed film can be defined as

$$\delta\epsilon = e(\theta_e) - \mu_\circ. \tag{14}$$

On a potassium substrate, $\delta\epsilon$ can be extrapolated, based on the results shown in Fig. 8, to something like 0.1 K (at the most). Clearly, such a small value is comparable to the overall accuracy of the VPI calculation, which is limited by the finite size of the simulated system, as well as by the uncertainties affecting the potentials utilized (primarily the substrate-adatom potential). If one compares this result with a binding energy of ~ 5 K on Li and ~ 2 K on Na, one might tentatively conclude that K is the "borderline" system for Helium adsorption, and that no stable film can form on an even weaker substrate.

The next weaker substrate is Rb, for which the situation is experimentally controversial.[5,7,11,14,15] A theoretical study,[23] based on DFT and making use of the same DF utilized here, proposed that a stable ^{4}He film should exist, at a coverage $\theta_e \sim 1$ Å^{-2}. The binding energy $\delta\epsilon$ of ^{4}He atom in such a film would be as little as ~ 0.03 K. Attempting to verify this result with VPI simulations would require performing calculations with at least five (and more likely ten) times as many atoms as in the largest system considered here (135 particles), which was not possible at this time, given the resources available for this project. Furthermore, one cannot help feeling skeptical as to whether the model and the potentials utilized can truly afford this type of precision.

We have nonetheless computed the ground-state energy per atom at low coverage. Results are shown in Fig. 9. VPI and DFT results agree to within ~ 0.1 K, with DFT once again underestimating e. We also note that at very low coverage ($\theta \lesssim 0.05$ Å^{-2}), DFT and VPI results diverge. The negative curvature of the energy data computed by VPI indicates that no stable uniform film exists at these coverage, which explains the disagreement with DFT, which has the assumption of a uniform film built-in.

V. DISCUSSION AND CONCLUSIONS

As noted above, the agreement between the results furnished by the two methods (VPI and DFT) is quite satisfactory, at least above the spinodal coverage, and is observed to improve with the weakening of the substrate, as stable films occur at greater values of θ; for example, the VPI and DFT estimates of the binding energy on a K substrate are the same, within the statistical error of VPI. One could tentatively make the reasonable assumption that the same type of agreement between VPI and DFT ought to be seen for Rb, at the coverage where a stable film might occur, according to DFT (namely ~ 0.44 Å^{-2}). As a result, VPI would confirm the DFT result of a stable ^{4}He film on Rb (i.e., wetting). At the same time, obviously a prediction of a binding energy of the order of a few hundreds of a K cannot be accepted without a serious critical analysis of the limitations affecting both calculations, as well as the starting point, namely the theoretical model utilized.

The systematic errors affecting the VPI calculation are attributable to the finite size of the simulated system, as well as the finite time step τ of the simulation and its length $L\tau$. Obviously, the last two sources of error can be reasonably accurately assessed by performing simulations of different length L and with different time steps. Less straightforward is the estimation of the size dependence of the results, as the computational cost roughly scales as the cubic power of the number of atoms, and it is usually impractical to carry out extensive simulations with significantly different values of N. However, because in this case one is dealing with systems that are essentially 2D, it is possible to gauge rather accurately the contribution to the potential energy arising from the periodic images of particles outside the main simulation cell (finite-size corrections on the kinetic energy are an order of magnitude smaller). We estimate the difference between our energy estimates and the values in the thermodynamic limit to be proportional to θ, and ~ 0.05 K in magnitude, for the largest coverage considered here (0.27 Å^{-2}). As this is of the order of the predicted binding energy on a Rb substrate, simulation on significantly larger systems are needed in order to address quantitatively the issue of a stable film.

Of course, one has to assess the realism and accuracy of the model (1), as well as of the potentials used in the calculation. The helium–helium potential used here is not the most recent version of the Aziz potential, but it is the one for which most of the many-body calculations based on quantum Monte Carlo have been carried out. In recent times, attempts to reproduce theoretically the equation of state of bulk liquid ^{4}He have been based on refined versions of the Aziz potential, with the explicit inclusion of three-body terms.[44] These are known to be quantitatively important in bulk superfluid Helium and are only *effectively* incorporated in the early ver-

sions of the Aziz potential. However, the Aziz potential used here reproduces rather accurately the equation of state of superfluid helium, and it is not clear whether the use of a more modern version of the potential in combination with a three-body potential would significantly change the results. More important seems the uncertainty of the substrate-adatom potential. The potentials used in this calculation are the most current and are a significant improvement over the early 3-9 potential, both with respect to the functional form as well as the value of the most important parameters (e.g., the well depth). However, their absolute accuracy has not yet been quantitatively assessed; to that aim, more experimental input will be needed.

Summarizing, we have carried out extensive ground-state quantum Monte Carlo simulations of adsorbed helium films on alkali metal substrates, using the most accurate potentials currently available. Comparison of the results obtained for the same problem using a density functional approach based on the Orsay-Trento functional shows good quantitative agreement; in particular, the values of equilibrium and spinodal coverage, as well as density profiles determined with the two methods are in excellent quantitative agreement. Only at very low coverage (below the spinodal) do the two calculations deviate from each other. At such low coverage, a uniform film is unstable against density fluctuations, and the uniform solution sought by density functional theory is not physically relevant. Results show stable ^{4}He films on Li, Na, and K substrates, with continuous film growth as a function of the chemical potential. On Li, a stable superfluid monolayer is found, in agreement with a previous theoretical calculation. On Na and K substrates, the lowest coverages for which stable films form correspond to effective thicknesses of two and four layers. Finally, on a Rb substrate, VPI data presented here do not allow us to draw a definitive conclusion, regarding the occurrence of a stable adsorbed film at $T=0$.

ACKNOWLEDGMENTS

This work was supported in part by the Petroleum Research Fund of the American Chemical Society under research Grant No. 36658-AC5 and by the Ministerio de Cultura y Educación of Argentina under research Grants ANCPyT No. PICT2000-03-08540 and UBACyT No. X103.

[1] See, for instance, L. W. Bruch, M. W. Cole, and E. Zaremba, *Physical Adsorption: Forces and Phenomena* (Clarendon Press, Oxford, 1997).
[2] P.-J. Nacher and J. Dupont-Roc, Phys. Rev. Lett. **67**, 2966 (1991).
[3] J. Rutledge and P. Taborek, Phys. Rev. Lett. **69**, 937 (1992).
[4] K. S. Ketola, S. Wang, and R. B. Hallock, Phys. Rev. Lett. **68**, 201 (1992).
[5] N. Bigelow, P. J. Nacher, and J. Dupont-Roc, J. Low Temp. Phys. **89**, 135 (1992).
[6] P. Taborek and J. E. Rutledge, Physica B **197**, 283 (1994).
[7] G. Mistura, H. C. Lee, and M. H. W. Chan, Physica B **194-196**, 661 (1994).
[8] B. Demolder, N. Bigelow, and J. Dupont-Roc, J. Low Temp. Phys. **98**, 91 (1995).
[9] R. B. Hallock, J. Low Temp. Phys. **101**, 31 (1995).
[10] E. Rolley and C. Guthmann, J. Low Temp. Phys. **108**, 1 (1995).
[11] A. F. G. Wyatt, J. Klier, and P. Stefanyi, Phys. Rev. Lett. **74**, 1151 (1995).
[12] J. Klier, P. Stefanyi, and A. F. G. Wyatt, Phys. Rev. Lett. **75**, 3709 (1995).
[13] D. Ross, J. E. Rutledge, and P. Taborek, Phys. Rev. Lett. **76**, 2350 (1996).
[14] J. A. Phillips, D. Ross, P. Taborek, and J. Rutledge, Phys. Rev. B **58**, 3361 (1998).
[15] T. A. Moreau and R. B. Hallock, J. Low Temp. Phys. **110**, 659 (1998).
[16] E. Cheng, M. W. Cole, W. F. Saam, and J. Treiner, Phys. Rev. Lett. **67**, 1007 (1991).
[17] E. Cheng, M. W. Cole, and J. Dupont-Roc, Rev. Mod. Phys. **65**, 557 (1993).
[18] B. E. Clements, E. Krotscheck, and H. J. Lauter, Phys. Rev. Lett. **70**, 1287 (1993).
[19] B. E. Clements, H. Forbert, E. Krotscheck, and M. Saarela, J. Low Temp. Phys. **95**, 849 (1994).
[20] F. Dalfovo, A. Lastri, L. Pricaupenko, S. Stringari, and J. Treiner, Phys. Rev. B **52**, 1193 (1995).
[21] See, for instance, F. Dalfovo, A. Lastri, and S. Stringari, in *Condensed Matter Theories*, edited by M. Casas, M. de Llano, J. Navarro, and A. Polls (Nova Science Publ., New York, 1995), Vol. 10, p. 469.
[22] F. Ancilotto, F. Faccin, and F. Toigo, Phys. Rev. B **62**, 17 035 (2000).
[23] L. Szybisz, Eur. Phys. J. B **14**, 733 (2000).
[24] L. Szybisz, Phys. Rev. B **62**, 3986 (2000); *ibid.* **62**, 12 381 (2000).
[25] L. Szybisz, Phys. Rev. B **67**, 132505 (2003).
[26] A. Chizmeshya, M. W. Cole, and E. Zaremba, J. Low Temp. Phys. **110**, 677 (1998).
[27] See, for instance, D. M. Ceperley, Rev. Mod. Phys. **67**, 279 (1995).
[28] M. Boninsegni and M. W. Cole, J. Low Temp. Phys. **113**, 393 (1998).
[29] M. Boninsegni, M. W. Cole, and F. Toigo, Phys. Rev. Lett. **83**, 2002 (1999).
[30] L. Szybisz and M. Boninsegni, J. Low Temp. Phys. **134**, 327 (2004).
[31] Lest the reader be misled by the use of the adjective "Variational," it is important to clarify at the outset that VPI is, just like PIMC, a numerically *exact* method, statistical and systematic errors being reducible as desired (at least in principle).
[32] R. A. Aziz, V. P. S. Nain, J. S. Carley, W. L. Taylor, and G. T. McConville, J. Chem. Phys. **70**, 4330 (1979).
[33] E. Zaremba and W. Kohn, Phys. Rev. B **13**, 2270 (1976).
[34] M. E. Pierce and E. Manousakis, Phys. Rev. B **62**, 5228 (2000).
[35] See, for instance, A. Sarsa, K. E. Schmidt, and W. R. Magro, J.

Chem. Phys. **113**, 1366 (2000).
[36] See, for instance, S. Jang, S. Jang, and G. A. Voth, J. Chem. Phys. **115**, 7832 (2001).
[37] Strictly speaking, Ψ_T is required to be nonorthogonal to the true ground-state wave function. For a Bose system this is not a problem, as the ground-state wave function can always be chosen real and positive, and therefore, any positive-definite function Ψ_T satisfies the nonorthogonality requirement. It is also necessary for Ψ_T to be non-negative, in order for (4) to be treated as a probability.
[38] S. Baroni and S. Moroni, Phys. Rev. Lett. **82**, 4745 (1999).
[39] S. Giorgini, J. Boronat, and J. Casulleras, Phys. Rev. B **54**, 6099 (1996).
[40] M. C. Gordillo and D. M. Ceperley, Phys. Rev. B **58**, 6447 (1998).
[41] The pair correlation function for a purely 2D ^{4}He system at coverage 0.052 Å^{-2} was computed separately by VPI in this project.
[42] J. M. Kosterlitz and D. J. Thouless, Prog. Low Temp. Phys. **78**, 371 (1978).
[43] See, for instance, Ref. 27; the same value was reproduced in this work, by means of VPI simulations for bulk ^{4}He.
[44] S. Moroni, F. Pederiva, S. Fantoni, and M. Boninsegni, Phys. Rev. Lett. **84**, 2650 (2000).